PERGAMON

International Journal of Multiphase Flow 28 (2002) 1333–1350

International Journal of Multiphase Flow

www.elsevier.com/locate/ijmulflow

Translational velocities of elongated bubbles in continuous slug flow

R. van Hout, D. Barnea, L. Shemer *

Department of Fluid Mechanics and Heat Transfer, Faculty of Engineering Tel-Aviv University, Tel-Aviv 69978, Israel

Received 26 February 2001; received in revised form 27 March 2002

Abstract

The translational velocities of elongated bubbles in continuous slug flow were measured for various flow rates, pipe inclinations and pipe diameters. Measurements were carried out by cross-correlating the output signals of consecutive optical fiber probes and by image processing technique. In addition, the velocities of single elongated bubbles in a stagnant and in a flowing liquid were measured by the same techniques. For all cases the measured velocities were compared to appropriate correlations. The measured velocities of single elongated bubbles were in all cases predicted quite well by the correlations while the velocities in continuous slug flow, for certain cases, were considerably underpredicted. This discrepancy is ascribed to the influence of the dispersed bubbles in the liquid slug region. A simplified model is proposed to calculate the translational velocity in continuous slug flow. The results of the model compare well with the measured translational velocities of elongated bubbles in continuous slug flow.

Keywords: Two-phase pipe flow; Slug flow; Translational velocity; Drift velocity; Fiber probe

1. Introduction

Gas–liquid slug flow is highly complex with an inherent unsteady behavior. It is characterized by large elongated bubbles separated by liquid slugs that may be aerated by small dispersed bubbles. The translational velocity of a single elongated bubble in a pipe has been studied extensively over the years and it is generally assumed that the translational velocity in a flowing liquid is a superposition of the bubble velocity in a stagnant liquid, i.e. the drift velocity U_d, and a contribution due to the mean liquid velocity, U_L, as proposed by Nicklin et al. (1962):

* Corresponding author. Tel.: +972-3-640-8128; fax: +972-3-740-7334.
E-mail address: shemer@eng.tau.ac.il (L. Shemer).

0301-9322/02/$ - see front matter
PII: S0301-9322(02)00027-7

$$U_{tr} = CU_L + U_d. \tag{1}$$

The value of the constant C is based upon the assumption that the propagation velocities of the bubbles follow the maximum local liquid velocity U_{max} in front of the nose tip (Nicklin et al., 1962; Bendiksen, 1984; Shemer and Barnea, 1987; Polonsky et al., 1999). Therefore $C = U_{max}/U_{mean}$, where U_{mean} is the mean cross-sectional liquid velocity. The parameter C equals approximately 1.2 for fully developed turbulent flow and 2.0 for laminar flow.

In vertical and horizontal pipes, the drift velocity U_d has been determined by potential flow analysis. Dumitrescu (1943) found that in vertical flow the Froude number Fr based on the drift velocity U_d^v equals:

$$Fr = U_d^v \Big/ \sqrt{gD} = 0.35, \tag{2}$$

where g is the gravitational constant and D is the pipe diameter. This agrees well with the experimental observations of Nicklin et al. (1962). In horizontal flow, Benjamin (1968) obtained that the Froude number based on the drift velocity, U_d^h , is

$$Fr = U_d^h \Big/ \sqrt{gD} = 0.54. \tag{3}$$

For the inclined case one has to rely upon experimental data. It was found experimentally (Zukoski, 1966; Bendiksen, 1984; Hasan and Kabir, 1986; Weber et al., 1986; Carew et al., 1995) that the maximum drift velocity occurs at an intermediate angle of inclination between $40° < \beta < 60°$ from the horizontal. Zukoski (1966) performed a comprehensive experimental investigation on the effects of the liquid viscosity μ, surface tension σ and pipe inclination β on the motion of single elongated bubbles in stagnant liquid for different pipe diameters ranging between $0.005 \leqslant D \leqslant 0.178$ m. The propagation rates were independent of viscous effects for $Re = \rho U_d D/\mu > 400$, where ρ is the liquid density. However, the propagation rates for inclined pipes depend on the surface tension parameter, $\Sigma = 4\sigma/\Delta\rho g D^2$, where $\Delta\rho$ is the density difference between liquid and gas phases.

The maximum in the drift velocity observed at $40° < \beta < 60°$ was explained qualitatively by Bonnecaze et al. (1971). They argued that the gravitational potential that drives the liquid velocity along the curved surface at the bubble nose first increases and then decreases as the angle of inclination varies from the vertical towards the horizontal position.

Bendiksen (1984) studied the propagation velocities of single elongated bubbles in flowing liquids at different inclination angles. The obtained velocities were plotted against the liquid velocity for each inclination angle. The drift velocities were then determined by extrapolation of the data to zero liquid velocity. The agreement between these drift velocities and those measured directly by Zukoski (1966) in stagnant liquid at the appropriate surface tension parameter was within 1%. The drift velocity for inclined flows has been correlated by Bendiksen (1984) as a weighted superposition of the drift velocity in vertical and horizontal flow:

$$U_d(\Sigma, \beta) = U_d^h(\Sigma, \alpha_B)\cos\beta + U_d^v(\Sigma, \alpha_B)\sin\beta, \tag{4}$$

where α_B is the void fraction in the film region of the elongated bubble. The values of U_d^h and U_d^v in Eq. (4) can be determined according to Zukoski (1966).

Alves et al. (1993) modeled the drift velocity in inclined flow using inviscid flow theory and taking the surface tension effects into consideration. The model results were compared with their

own experimental data and with the data of Zukoski (1966). In general, the model shows a good agreement with the experiment.

The dependence of the factor C in Eq. (1) on the inclination angle, $C = C(\beta)$ was also measured by Bendiksen (1984) for different ranges of liquid flow rates in a pipe of $D = 0.0242$ m. For relatively low liquid flow rates, $Fr_L = U_L/(gD)^{1/2} < 3.5$ and $Re_L = \rho U_L D/\mu > 6000$, $C(\beta)$ was correlated by

$$C(\beta) = C(0^\circ) + [C(90^\circ) - C(0^\circ)]\sin^2\beta, \tag{5}$$

where $C(0^\circ) = 1$ and $C(90^\circ) = 1.2$.

A large volume of data on propagation velocities of a single elongated bubble has thus been accumulated over the years. In contrast, propagation velocities in continuous slug flow are much less documented. Nicklin et al. (1962) proposed to use correlation (1), obtained for a single elongated bubble in a flowing liquid, for continuous slug flow as well, while substituting the mean liquid velocity U_L by the mixture velocity U_m:

$$U_{tr} = CU_m + U_d, \tag{6}$$

where $U_m = U_{LS} + U_{GS}$, U_{LS} and U_{GS} being the liquid and gas superficial velocities.

Few comparisons were made to validate the use of Eq. (6) for the calculation of translational velocities of elongated bubbles in continuous slug flow. Fernandes et al. (1983) and Mao and Dukler (1989) measured the propagation velocities of Taylor bubbles in vertical upward, continuous slug flow in a 0.05 m pipe. In both cases the measured velocities were underpredicted by using Eq. (6) with $C = 1.2$. The value of $C = 1.29$ was thus adopted. Legius et al. (1997) performed measurements of U_{tr} in continuous vertical upward slug flow in a 0.05 m internal diameter pipe. Measurements were carried out 7 m ($L/D = 140$) from the inlet using three different measurement methods. An excellent agreement was claimed between Eq. (6) and the measured translational velocities. Unfortunately, no comparison was made between the different measurement methods and it is not clear how the presented velocities were averaged and what are the typical ensemble sizes. No information is available regarding the applicability of Eq. (6) to inclined continuous slug flow.

The present investigation is aimed at clarifying the conditions for which the use of Eq. (6) for the prediction of the translational velocities in continuous slug flow is appropriate. The translational velocities of elongated bubbles in continuous slug flow as well as of single elongated bubbles in a stagnant and in a flowing liquid, are measured and compared to the existing correlations. A simplified model for the calculation of the translational velocity in continuous slug flow is presented.

2. Experimental facility and data processing

2.1. Experimental facility

The experimental facility consists of two 10 m long, parallel transparent Perspex pipes with internal diameters of $D = 0.024$ and 0.054 m. The system can be rotated around a horizontal axis to any inclination in the range $0^\circ \leqslant \beta \leqslant 90^\circ$.

The gas and the liquid superficial velocities are measured by a set of rotameters. Air is supplied from a central line via a pressure reducer adjusted to 0.1 MPag within the rotameter. The inlet valve used to adjust the gas flow rate is located downstream of the rotameter. The test pipes are open to the atmospheric pressure at the exit and the volumetric gas flow rate measured by the rotameters is converted to standard atmospheric conditions. The gas flow rates presented in the following figures relate to the conditions prevailing at the exit. Since the gas superficial velocity increases along the pipe due to gas expansion, the effective gas superficial velocity at the measurement position was recalculated by taking into account the pressure drop along the pipe (Barnea, 1990). The mixture velocity at the measurement position U_m, Eq. (6), was adjusted accordingly. Tap water filtered by an ion exchanger is circulated in a closed loop through the system by a centrifugal pump. Air and water are introduced through a "mixer"-type inlet device, which is 0.3 m long. The values of the surface tension parameter $\Sigma = 4\sigma/\Delta\rho g D^2$ are $\Sigma = 0.052$ for $D = 0.024$ m and $\Sigma = 0.010$ for $D = 0.054$ m. More details on the experimental facility can be found in van Hout et al. (2001).

2.2. Measurement techniques and data processing

Measurements of the bubble interface velocities were carried out using optical fiber probes and image processing technique.

Optical fiber probes: Up to three optical fiber probes (Photonetics) with sensitive probe tip diameter of 0.14 mm were used simultaneously. The stainless steel probe body protecting the silica fiber has an outer diameter of 3 mm and an immersable length up to 200 mm. The silica fiber extends unprotected 10 mm from the stainless steel probe body. The probes were mounted on a specially constructed module at axial distances of 0.020 m. A traversing mechanism allowed accurate positioning of the sensitive probe tips at any desired radial position within the pipe (van Hout et al., 2001).

The return signals of the optical fiber probes were sampled by an A/D converter at a sampling frequency of $f_S = 1$ kHz per probe and sampling duration $t_S = 3600$ s. The times where a transition was made from gas to liquid or vice versa, relative to the sampling start, were called the "transition times". Between two successive transitions no changes occurred and extra sampling points between them were redundant. The transition times were stored in a data file. An example of the raw output signals of two consecutive optical fiber probes at an axial distance of 0.040 m is shown in Fig. 1(a). A value of 2048 corresponds to the gas phase and 0 corresponds to the liquid phase. These signals indicate clearly the difference between the elongated bubble zone (EB) and the liquid slug zone (LS). The EB is characterized by a long gas duration while the LS is the region between two elongated bubbles where gas/liquid and liquid/gas transitions frequently occur due to the small bubbles that are dispersed in the liquid slug. Note the similarity of the output signals for the two probes, mounted a small axial distance apart. Residence times of the phases over the probe tip were determined from successive transition times. Length information was obtained by multiplication of these residence times by appropriate velocities.

The different gas phase duration scales in the EB and LS allow filtering of the raw output signals. A threshold for the minimum elongated bubble length, $\ell_{th} = 1D$, was chosen and the corresponding minimum elongated bubble duration was found by multiplication of ℓ_{th} by the characteristic translational velocity determined by the cross-correlation of the raw probe signals.

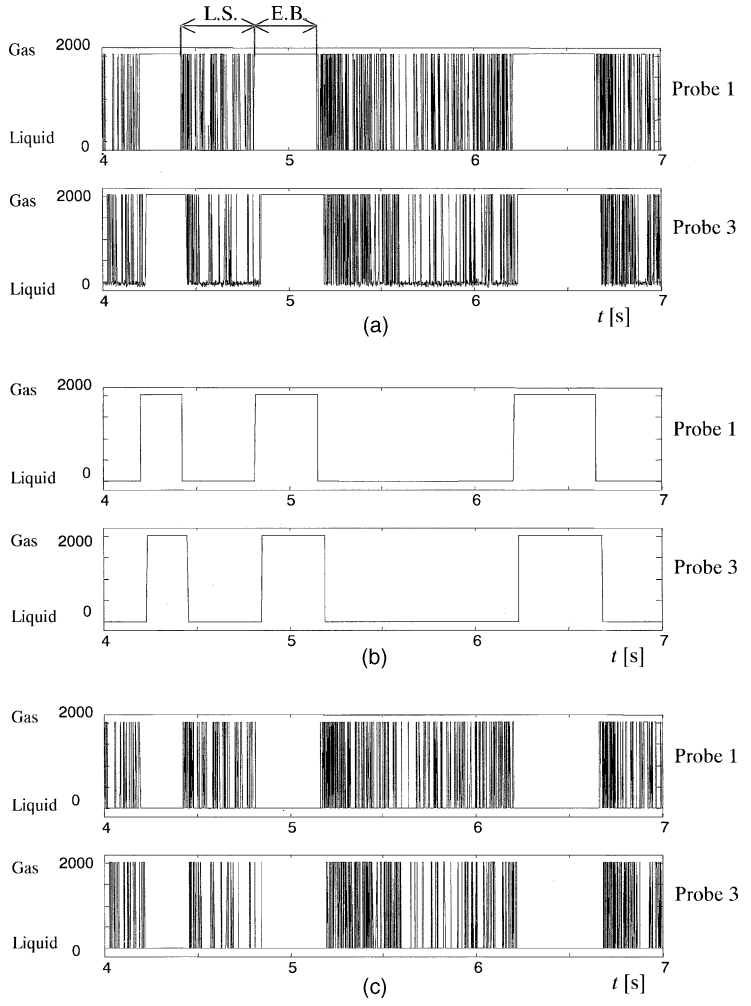

Fig. 1. Output signals for two consecutive optical fiber probes. (a) Raw TTL signal. (b) EB TTL signal, elongated bubbles only. (c) DB TTL signal, dispersed bubbles in liquid slug.

Two types of filtered signals were obtained, one containing only the elongated bubbles (Fig. 1(b), EB TTL signals) and the other only the dispersed bubbles in the liquid slug (Fig. 1(c), DB TTL signals). The most probable interface velocities of both the elongated bubbles and the dispersed bubbles were determined using a direct cross-correlation technique of the filtered signals from two successive probes (Bendat and Piersol, 1968). Typical examples of the obtained cross-correlation curves both for the EB TTL signals and the DB TTL signals are shown in Fig. 2(a) and (b) respectively at different inclination angles. The axial distance between the two probe tips is 0.020 m. The cross-correlation coefficient is depicted as a function of the time lag. The most probable time lag for a bubble to move from one probe to the other corresponds to the maximum cross-correlation coefficient. It can be seen that this time lag depends on the inclination angle. Moreover, the maximum values of the cross-correlation coefficient increase with decreasing inclination

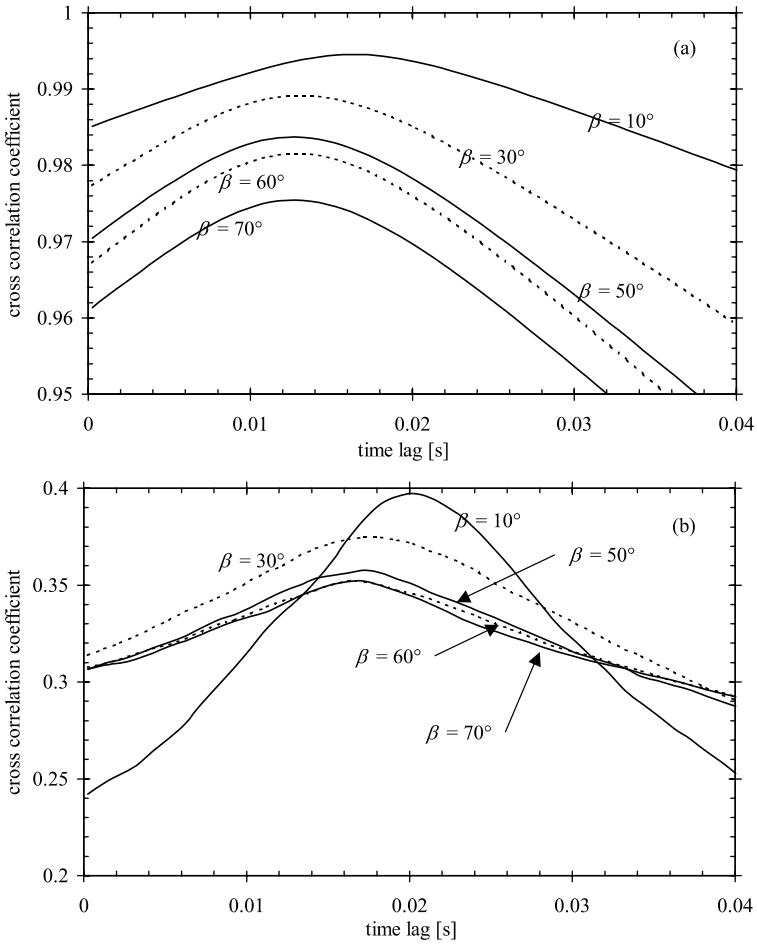

Fig. 2. Cross-correlation coefficient as a function of time lag for different inclination angles. $D = 0.054$ m. $U_{LS} = 0.10$ m/s, $U_{GS} = 0.63$ m/s. (a) EB TTL signals. (b) DB TTL signals.

angle. This can be attributed to lower bubble distortion and less aerated liquid slugs observed for smaller inclination angles. The most probable time lag and the distance between the probes yield the characteristic velocity of the elongated and of the dispersed bubbles. Furthermore, it can be seen in Fig. 2 that the maximum cross-correlation coefficient for the EB TTL signal is close to unity suggesting a highly coherent signal, whereas for the dispersed bubbles its value is much lower. In continuous slug flow, the cross-correlation technique does not distinguish between the nose and tail velocity of an elongated bubble and determines an average between them. For the single bubble measurements, however, care was taken to only perform cross correlation on the rising edge of the probe signals (i.e. the bubble nose). In this case the determined velocity is the bubble nose velocity.

Image processing: The aim of the image processing technique is to visualize the air–water interfaces in order to obtain quantitative information on the interface velocities. Series of images of the flow (640 × 480 pixels) taken by a video camera were digitized by a frame-grabber board and

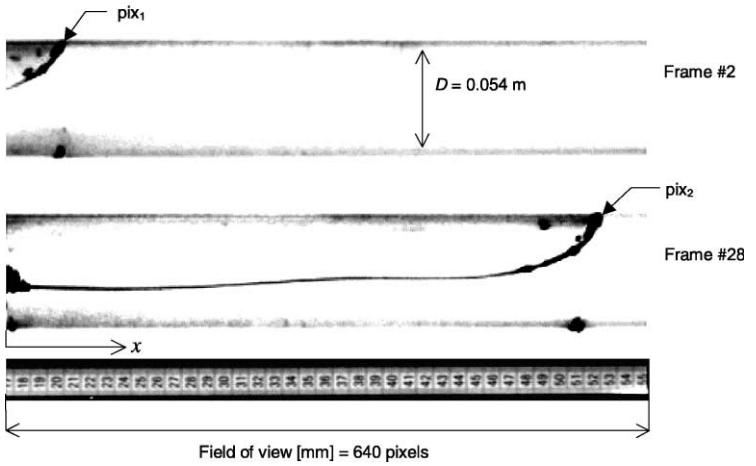

Fig. 3. Determination of the elongated bubble velocity by image processing technique. Example for stagnant liquid, $\beta = 10°$, frame numbers 2 and 28. Frame rate = 60 fps.

processed by specialized software. The images were contrast enhanced to clearly discern the air–water interfaces. The determination of the interface velocity according to the bubble nose is illustrated in Fig. 3. The axial position in pixels of the elongated bubble interface was determined upon entering the field of view of the camera (pix_1) and leaving it (pix_2). The pixelsize (mm/pixel) was calculated by dividing the field of view of the camera (mm) by the number of pixels in the x-direction. The camera was operated in an interlaced mode at a frame rate of 30 fps (NTSC). After deinterlacing, the effective frame rate is 60 fps (Polonsky et al., 1999). The interface velocity is given by

$$U_{\mathrm{tr}} = \frac{|\mathrm{pix}_1 - \mathrm{pix}_2|}{\Delta_{\mathrm{frames}}} \text{ pixelsize (60 fps)}, \tag{7}$$

where Δ_{frames} is the number of frames elapsed between bubble entering and leaving the field of view of the camera. Usually Δ_{frames} was in the range from 20 to 30.

2.3. Experimental conditions

Bubble velocity measurements were carried out on single elongated bubbles as well as in continuous slug flow using both image processing and optical fiber probes. For 90° upward flow, the optical fiber probe tips were located at the centerline of the pipes, while for inclined flow the probes were mounted in the upper part of the pipe (at $y = 6.5$ mm for $D = 0.054$ m and at $y = 6$ mm for $D = 0.024$ m, where y is measured from the upper wall of the pipe). The experiments using optical fiber probes were carried out at $x/D = 127$ for $D = 0.054$ m and at $x/D = 287$ for $D = 0.024$ m. The video camera was located in all cases at 7.9 m from the pipe inlet corresponding to $x/D = 146$ for $D = 0.054$ m and $x/D = 329$ for $D = 0.024$ m.

Single bubble injection was carried out in stagnant liquid and in co-flowing liquid. To inject a single bubble in stagnant liquid, the pipe was first filled with water and set to the desired

inclination angle. The water pump was shut down and the entry water valve was closed manually. Care was taken to assure that residual disturbances had disappeared before injecting a bubble. Injection was carried out manually by opening and closing the gas inlet valve. Expansion effects were negligible (Polonsky et al., 1999). Initial disturbances due to the bubble injection decayed fast and did not affect the bubble motion at the measurement position. Bubble injection in co-flowing liquid was carried out in a similar way. At each inclination angle five bubbles were injected. In stagnant liquid, measurements were carried out using both image processing technique and optical fiber probes at various inclination angles ranging from 2° to 90°. In a co-flowing liquid, experiments were carried out by image processing technique only at two liquid flow rates for each pipe diameter. The liquid flow rates were selected so that they corresponded to the mixture velocity U_m in some of the continuous slug flow experiments. Measurements were carried out at inclinations ranging from 0° to 60°.

In continuous slug flow, experiments were carried out for various gas and liquid flow rates and inclination angles ranging from 2° to 90°. The return signals of the optical probes were sampled for a duration $t_S = 3600$ s, resulting in a large ensemble size (order of 10^3). In the experiments using image processing technique, 30–40 different elongated bubbles were taken into account.

3. Experimental results

The purpose of the present experiments is to address the open question regarding the relevance of the data obtained for the translational velocities of single elongated bubbles to the prediction of the translational velocities of bubbles in continuous slug flow. To this end, a systematic study of the velocities of elongated bubbles was performed, starting with measurements of the translational velocity of single bubbles in stagnant liquid and extended to single elongated bubbles in co-flowing liquid. Then, the translational velocities of elongated bubbles in continuous slug flow were determined and compared to those obtained for single bubbles. In our experiments U_d^v does not depend on Σ ($\Sigma < 0.10$ for both pipes, Zukoski, 1966) and is calculated by Eq. (2). In contrast, U_d^h depends on Σ and is obtained according to Zukoski (1966) at the corresponding Σ: $U_d^h = 0.18$ m/s for $D = 0.024$ m and $U_d^h = 0.33$ m/s for $D = 0.054$ m. These values of U_d^v and U_d^h were used here to calculate the drift velocity according to Eq. (4).

3.1. Translational velocity of single elongated bubbles

The dimensionless drift velocity, expressed by the Froude number, $U_d/(gD)^{1/2}$, is shown in Fig. 4 for both $D = 0.024$ and 0.054 m as a function of the pipe inclination angle β. In this figure the experimental results for the drift velocity of single elongated bubbles obtained by the image processing technique and by the optical fiber probes are presented and compared to the data of Zukoski (1966) and the predictions by Bendiksen (1984) and Alves et al. (1993). In addition, the drift velocities estimated for continuous slug flow are also shown in Fig. 4(b) and will be discussed in sequel. The absolute error of the measurements by the optical fiber probes is within 5% whereas the accuracy of the image processing technique is given by the standard deviation that does not exceed 3%.

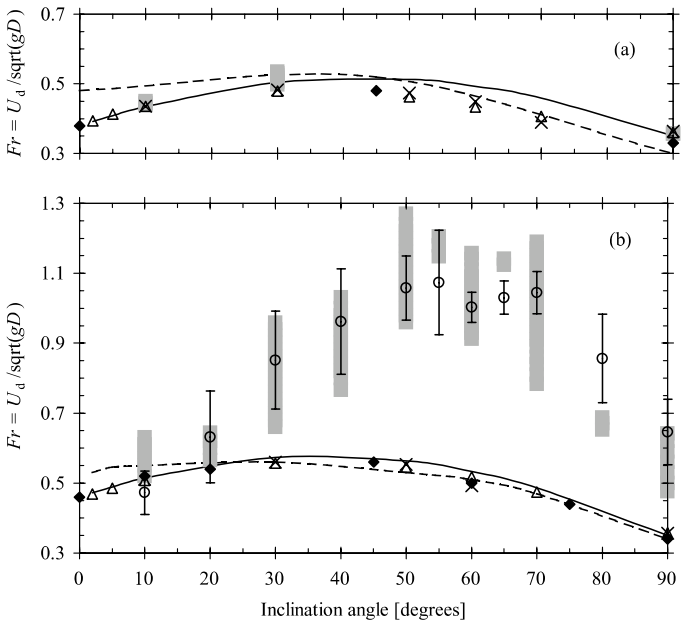

Fig. 4. Froude number based on the drift velocity as a function of inclination angle. (a) $D = 0.024$ m; $\Sigma = 0.052$; (b) $D = 0.054$ m; $\Sigma = 0.010$. (◆) Zukoski (1966); (—) Bendiksen (1984); (- - -) Alves et al. (1993). *Single bubble data*: (△) image processing; (×) optical probes. *Continuous slug flow*: (○) Data-extrapolation, bars represent std. error; (▮) Model-range of $U_{d,eff}$, Eq. (10).

The results obtained by both experimental methods for single elongated bubbles show an excellent agreement. The drift velocity has a maximum for $30° < \beta < 50°$. Furthermore, it can be seen that the current data compare well with the measurements of Zukoski (1966) at the appropriate value of Σ. The model of Alves et al. (1993) compares well with the experimental data for $\beta > 30°$. For smaller inclination angles, this model somewhat overpredicts the experimental results. The drift velocity given by the Bendiksen correlation (4) (solid line) agrees well with the experimental data for both pipe diameters over the whole range of pipe inclinations.

The translational velocity, U_{tr}, of a single elongated bubble in a co-flowing liquid measured by the image processing technique is presented in Fig. 5 for both pipe diameters as a function of the inclination angle. The error bars indicate the standard deviation. A comparison is made with the predicted velocities according to the Nicklin correlation (1), using the drift velocity given by Eq. (4). Two curves according to Eq. (1) are shown. For one curve, the parameter C equals 1.2, while for the other curve, C depends on the inclination angle according to Eq. (5) (Bendiksen, 1984). The Nicklin correlation with a constant C slightly overpredicts the measured translational velocities at decreasing inclination angles. Application of Eq. (5) to account for the dependency of $C = C(\beta)$ improves the agreement. In general, the translational velocities of single elongated bubbles in inclined co-flowing liquids are well predicted by Eq. (1) with the use of Eq. (4) for U_d. The validity of these relations for continuous slug flow is investigated in sequel.

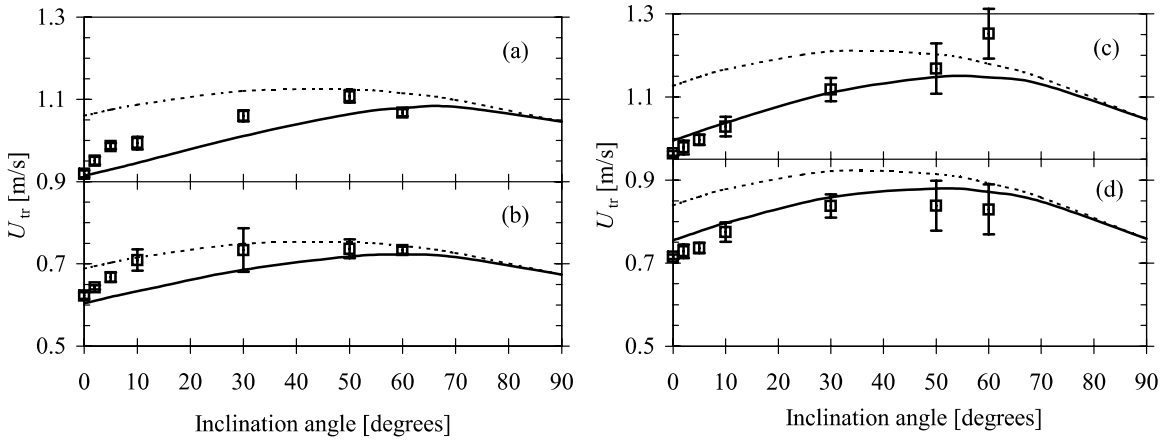

Fig. 5. Translational velocity U_{tr} of a single bubble in a co-flowing liquid as a function of inclination angle. (a) $U_m = U_L = 0.73$ m/s, $D = 0.024$ m; (b) $U_m = U_L = 0.42$ m/s, $D = 0.024$ m; (c) $U_m = U_L = 0.66$ m/s, $D = 0.054$ m; (d) $U_m = U_L = 0.42$ m/s, $D = 0.054$ m. (- - -) Eq. (1), $C = 1.2$; (—) Eq. (1), $C = f(\beta)$; (□) image processing.

3.2. Translational velocities of elongated bubbles in continuous slug flow

The measured translational velocities of elongated bubbles in developed continuous slug flow as a function of the inclination angle are shown in Fig. 6 for $D = 0.024$ m and in Fig. 7 for $D = 0.054$ m. A good agreement is obtained between the results obtained by the image processing technique and by the optical fiber probes. The accuracy of the velocities determined by the image processing technique is given by the error bars based on the standard deviation. The standard deviations increase with β as the elongated bubble behavior becomes much more complex. It should be

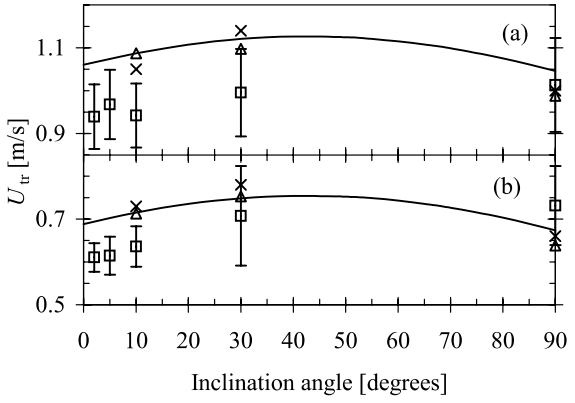

Fig. 6. Translational velocities of elongated bubbles in continuous slug flow as a function of inclination angle. $D = 0.024$ m. (a) $U_{LS} = 0.10$ m/s; $U_{GS} = 0.63$ m/s. (b) $U_{LS} = 0.01$ m/s; $U_{GS} = 0.41$ m/s. (×) Optical fiber probes; (—) Eq. (6); (□) image processing; (Δ) $U_{tr,eff}$, Eq. (11).

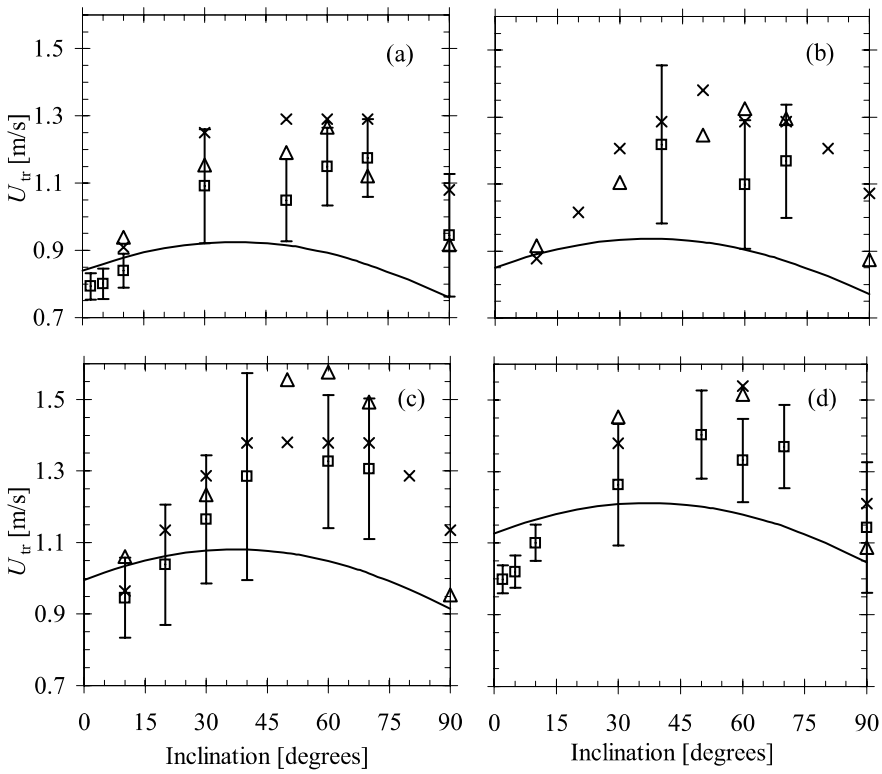

Fig. 7. Translational velocities of elongated bubbles in continuous slug flow as a function of inclination angle. $D = 0.054$ m. (a) $U_{LS} = 0.01$ m/s; $U_{GS} = 0.41$ m/s. (b) $U_{LS} = 0.09$ m/s; $U_{GS} = 0.34$ m/s. (c) $U_{LS} = 0.21$ m/s; $U_{GS} = 0.34$ m/s. (d) $U_{LS} = 0.25$ m/s; $U_{GS} = 0.41$ m/s. (×) Optical fiber probes; (—) Eq. (6); (□) image processing; (Δ) $U_{tr,eff}$ Eq. (11).

remembered that quantitative image processing is quite cumbersome. When carried out on images acquired in continuous slug flow, the elongated bubble nose interface is often hard to detect due to the highly aerated liquid slug zone, especially for $\beta > 30°$. Application of the optical fiber probes is therefore advantageous for the determination of statistical parameters in continuous slug flow, allowing ensemble sizes of the order 10^3. The accuracy of the data obtained by the optical probes in this case is determined not only by the finite sampling frequency (as was the case for a single elongated bubble) but also by the spread in velocities naturally occurring in continuous slug flow, as well as by bubble distortion. More details can be found in van Hout (2001).

A snapshot of an elongated bubble rising in vertical upward co-current continuous slug flow is shown in Fig. 8 for $D = 0.054$ m. The liquid slug is densely aerated and the nose interface is highly distorted. Some of the dispersed bubbles are swept into the liquid film region. A crude balance of the gas flux moving downwards in the frame of reference of the elongated bubble shows that in the liquid film region the gas flux is smaller by two orders of magnitude than in the liquid slug and thus can be neglected in the gas mass balance at the elongated bubble nose.

In addition to the measured velocities, the predicted velocities by the Nicklin correlation (6) with $C = 1.2$ and U_d according to Eq. (4) are shown in Figs. 6 and 7. The measured translational

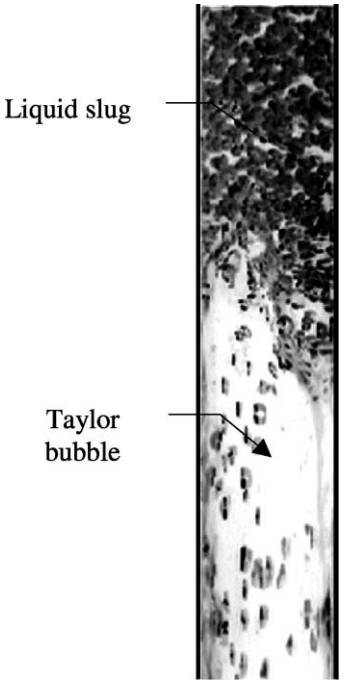

Fig. 8. A snapshot of an elongated bubble moving upwards in vertical continuous slug flow.

velocities for the small pipe diameter are quite well predicted by Eq. (6) (Fig. 6). In contrast to that, for the large pipe diameter, a substantial discrepancy between the measured velocities and those predicted by Eq. (6) is clearly observed (Fig. 7). The Nicklin correlation does not describe adequately neither the angular dependence nor the absolute values of the translational velocity in inclined slug flow for $D = 0.054$ m. It thus becomes important to look for the reasons that cause the observed disagreement between Eq. (6) and the experimental results.

We therefore analyze the dependence of the measured translational velocity of elongated bubbles in continuous slug flow on the mixture velocity, U_m. The drift velocity in continuous slug flow at each inclination angle can be extracted from extrapolating this dependence to $U_m \to 0$ (see Fig. 9). Both the data points and a linear fit (of the form $U_{tr} = CU_m + U_d$) are shown in this figure for $D = 0.054$ m. The standard deviation of the measured data points from the linear fit is in all cases smaller than 0.1 m/s and the R^2 value (measure of goodness of fit, Draper and Smith, 1998) in all cases exceeds 0.9. It can be seen that the value of C compares well with the generally used value of 1.2 in turbulent flow. No pronounced effect of β on the value of C can be detected.

The fact that the estimated value of the parameter C in continuous slug flow is close to 1.2 suggests that the observed difference between the measured elongated bubble velocities in continuous slug flow and those predicted by the Nicklin correlation (6), as observed in Fig. 7, can only be ascribed to inappropriate use of the drift velocities. In Fig. 4(b), the drift velocities obtained by extrapolation of U_{tr} vs. U_m in continuous slug flow are compared to the measured drift velocities of single bubbles. The error bars represent the standard error. For the large pipe di-

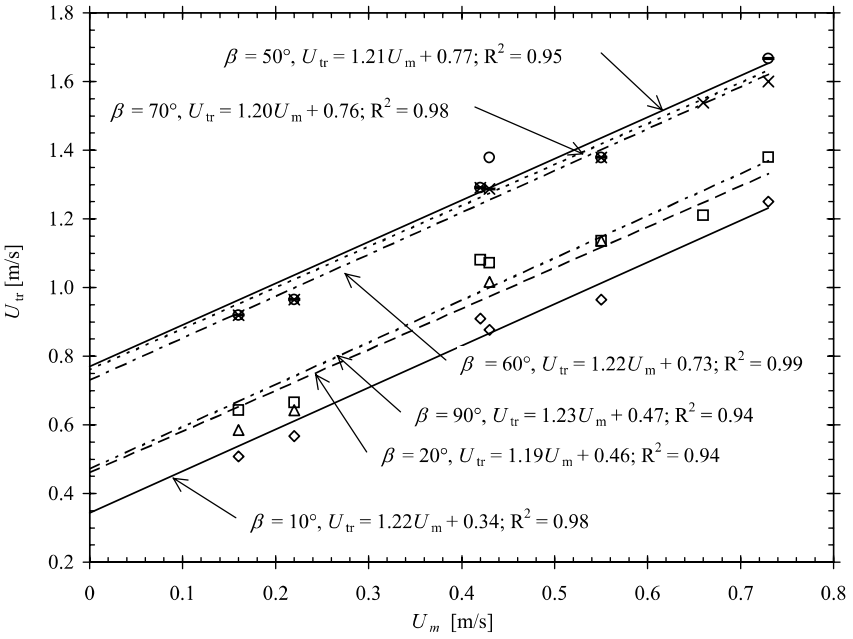

Fig. 9. Regression analysis on translational velocities measured by optical fiber probes. $D = 0.054$ m. (◇) 10°; (△) 20°; (○) 50°; (×) 60°; (–) 70°; (□) 90°.

ameter and for $\beta > 20°$, Fig. 4(b), the extrapolated drift velocities in continuous slug flow are significantly higher than those of single bubbles.

4. Model

The observed difference between the drift velocity of single elongated bubbles in stagnant liquid and the extrapolated drift velocity in continuous slug flow (Fig. 4) can be attributed to the presence of dispersed bubbles in the liquid slug region. When the dispersed bubbles in continuous slug flow propagate at a velocity that is lower than the translational velocity of the elongated bubbles, they coalesce with the elongated bubble at its nose. At the same time dispersed bubbles are created at the elongated bubble tail. The coalescence of the dispersed bubbles at the elongated bubble nose results in an effectively higher translational velocity of the elongated bubble.

For simplicity, consider a flat-nosed, cylindrical elongated bubble, propagating in stagnant liquid at a drift velocity U_d as shown in Fig. 10. In front of its nose, in the liquid slug region with a mean void fraction α_S, dispersed bubbles move at a drift velocity U_0. The increase of the elongated bubble drift velocity U_d, due to the dispersed bubble coalescence at the bubble front, can be estimated as follows.

In the absence of dispersed bubbles, the displacement of the elongated bubble nose position during a time interval Δt would be $\Delta x_1 = U_d \Delta t$. However, in the presence of dispersed bubbles and for $U_d > U_0$ dispersed bubbles are absorbed in the elongated bubble during the time interval Δt

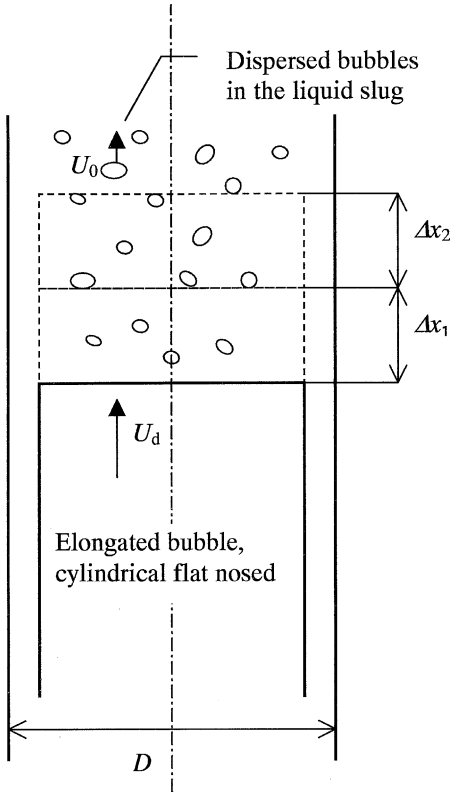

Fig. 10. A sketch for the model.

and the elongated bubble front is displaced by an additional increment Δx_2. The liquid film region around the elongated bubble is assumed to be free of dispersed bubbles. A simple mass balance at the elongated bubble front yields:

$$(\Delta x_1 + \Delta x_2)\alpha_S - U_0 \Delta t \alpha_S = \Delta x_2 \alpha_B, \tag{8}$$

where α_B is the average void fraction in the elongated bubble region. Thus

$$\Delta x_2 = \frac{\Delta x_1 \alpha_S - U_0 \Delta t \alpha_S}{\alpha_B - \alpha_S} \tag{9}$$

and the effective drift velocity $U_{d,eff} = \Delta x/\Delta t = (\Delta x_1 + \Delta x_2)/\Delta t$, is given by

$$U_{d,eff} = U_d + \frac{(U_d - U_0)\alpha_S}{\alpha_B - \alpha_S} \quad \text{for } U_d > U_0, \tag{10}$$

where the last term is the addition to the drift velocity of a single bubble due to the absorption of the dispersed bubbles at the elongated bubble nose in continuous slug flow. Note that this term vanishes when $\alpha_S = 0$ (no dispersed bubbles in the liquid slug) or when the elongated bubble drift velocity equals the drift velocity of the dispersed bubbles, $U_d = U_0$. When $U_d < U_0$, dispersed

bubbles are present only in the near wake region and are absent in the front of the trailing bubble. Hence, the void fraction in the liquid slug region, α_S, will eventually become negligible.

The effective translational velocity of elongated bubbles in continuous slug flow is thus given by

$$U_{tr,eff} = U_{tr,N} + \frac{(U_d - U_0)\alpha_S}{\alpha_B - \alpha_S} \quad \text{for } U_d > U_0, \tag{11}$$

where $U_{tr,N}$ is the predicted translational velocity of elongated bubbles by the Nicklin correlation (6).

The average void fraction in the liquid slug α_S was determined in the present work from the output signals of the optical fiber probes as the ratio between the sum of the gas durations in the liquid slug to the total liquid slug durations (Fig. 1), see van Hout et al., 1992. The drift velocities of single elongated bubbles propagating in stagnant liquid U_d were also measured in the present work (Fig. 4). Therefore, the remaining unknowns in Eq. (11) that were not measured directly, are the dispersed bubble drift velocity U_0 and the average void fraction in the elongated bubble region α_B.

The value of U_0 can be calculated as follows: the free rise (drift) velocity of a single dispersed bubble, $U_{0\infty}$, depends on the bubble diameter. When the bubble size exceeds some critical bubble value d_c, the drift velocity tends to be constant and independent of the bubble diameter. The critical bubble size d_c, is given by Brodkey (1967)

$$d_c \cong [0.4\sigma/\Delta\rho g]^{1/2}. \tag{12}$$

For an air/water flow this critical diameter is $d_c \approx 1.7$ mm, while in our facility the dispersed bubbles in the liquid slug are usually larger (Barnea and Shemer, 1989). The drift velocity of a bubble with $d > d_c$ is constant and can be estimated as (Harmathy, 1960):

$$U_{0\infty} = 1.54\left[\sigma g \Delta\rho/\rho^2\right]^{1/4}. \tag{13}$$

Furthermore, the drift velocity of a dispersed bubble within a swarm of bubbles is lower than the free rise velocity of a single bubble by a factor of $(1 - \alpha_S)^q$, where $q = 1.5$ (Wallis, 1969). For inclined pipes, the drift velocity is multiplied by $\sin\beta$ as proposed by Barnea and Brauner (1985). The dispersed bubble drift velocity, U_0, in inclined slug flow is thus

$$U_0 = U_{0\infty}(1 - \alpha_S)^q \sin\beta. \tag{14}$$

The value of the second unknown, α_B was determined from the available information on the average void fraction of a slug unit α_u, which is defined as:

$$\alpha_u = \alpha_S \frac{\ell_S}{\ell_u} + \frac{1}{\ell_u}\int_0^{\ell_B} \alpha_B \, dx, \tag{15}$$

where the length of a slug unit ℓ_u equals the elongated bubble length ℓ_B plus the liquid slug length ℓ_S. Applying mass balance equations, α_u can be presented as (Taitel and Barnea, 1990)

$$\alpha_u = (U_{GS} - U_b\alpha_s + U_{tr}\alpha_S)/U_{tr}. \tag{16}$$

Assuming an average constant value of α_B, Eqs. (15) and (16) yield the average void fraction in the elongated bubble region α_B:

$$\alpha_B = \alpha_S + \frac{(U_{GS} - U_b\alpha_S)\ell_u}{U_{tr}\ell_B}. \tag{17}$$

All terms on the right-hand side of Eq. (17) were measured directly in the present research (Table 1). The translational velocity of the elongated bubbles, U_{tr}, and the propagation velocity of the dispersed bubbles in the liquid slug, U_b, are measured by cross-correlating the EB TTL signals and DB TTL signals, respectively (Fig. 1(b) and (c)). The mean slug lengths ℓ_S and elongated bubble lengths ℓ_B are determined experimentally (van Hout et al., 2001). The values of α_B calculated from Eq. (17) are in agreement with the direct measurements of film thickness by van Hout et al. (1992).

The effective translational velocity $U_{tr,eff}$, can now be calculated from Eq. (11) for different inclination angles, flow conditions and pipe diameters. A comparison of $U_{tr,eff}$ to the measured translational velocities of elongated bubbles in continuous slug flow, U_{tr}, is presented in Table 1 for some flow rates. A comparison between the measured translational velocity U_{tr} and the predicted translational velocity in continuous slug flow, $U_{tr,eff}$, is shown in the last column of Table 1. It can be seen that the agreement between the measured and the predicted values is within 15%.

Table 1
Measured (optical probes) and calculated translational velocities of elongated bubbles in continuous slug flow

Inclination (°)	Measured parameters							Calculated parameters				
	U_{tr} (m/s)	U_b (m/s)	U_d (m/s)	α_s	U_{GS} (m/s)	ℓ_B (D)	ℓ_S (D)	U_0 (m/s)	α_B	$U_{d,eff}$ (m/s)	$U_{tr,eff}$ (m/s)	$\lvert U_{tr} - U_{tr,eff}\rvert / U_{tr}$ (%)
$D = 0.054$ m; $U_{LS} = 0.01$ m/s; $U_{GS} = 0.41$ m/s												
90	1.08	0.83	0.26	0.33	0.37	17.1	20.7	0.14	0.53	0.47	0.92	15.2
70	1.26	0.95	0.35	0.28	0.37	12.5	15.9	0.14	0.47	0.66	1.12	11.0
60	1.32	1.00	0.38	0.28	0.38	12.6	14.3	0.13	0.44	0.79	1.27	4.1
50	1.25	0.95	0.40	0.26	0.39	13.3	14.1	0.12	0.49	0.71	1.19	4.7
30	1.18	0.93	0.41	0.22	0.40	15.9	12.5	0.09	0.51	0.65	1.15	2.2
10	0.89	0.73	0.37	0.09	0.41	22.8	8.6	0.04	0.62	0.43	0.94	5.5
$D = 0.054$ m; $U_{LS} = 0.10$ m/s; $U_{GS} = 0.63$ m/s												
90	1.38	1.16	0.26	0.34	0.58	18.9	21.6	0.13	0.63	0.41	1.22	11.7
70	1.61	1.22	0.35	0.30	0.58	14.6	15.2	0.14	0.57	0.57	1.39	13.4
60	1.61	1.25	0.38	0.30	0.59	15.4	14.1	0.13	0.56	0.66	1.50	7.0
50	1.59	1.22	0.40	0.29	0.59	16.6	13.4	0.12	0.56	0.70	1.54	3.1
30	1.51	1.15	0.41	0.26	0.61	19.9	12.3	0.08	0.59	0.65	1.52	0.5
10	1.22	1.00	0.37	0.14	0.63	26.7	8.1	0.03	0.66	0.46	1.34	9.8
$D = 0.024$ m; $U_{LS} = 0.01$ m/s; $U_{GS} = 0.41$ m/s												
90	0.66	0.60	0.17	0.20	0.38	30.3	16.3	0.18	0.81	0.17	0.64	3.3
30	0.70	0.70	0.23	0.08	0.40	41.7	19.5	0.11	0.80	0.24	0.75	7.6
10	0.64	0.63	0.21	0.01	0.41	46.0	11.6	0.04	0.80	0.21	0.71	11.4
$D = 0.024$ m; $U_{LS} = 0.10$ m/s; $U_{GS} = 0.63$ m/s												
90	1.00	1.00	0.17	0.20	0.58	34.5	17.2	0.18	0.77	0.17	0.99	1.2
30	1.14	1.11	0.23	0.12	0.59	35.7	12.6	0.10	0.66	0.25	1.10	3.7
10	1.04	1.00	0.21	0.03	0.62	52.2	11.6	0.04	0.72	0.22	1.09	4.5

The Froude number based on the calculated effective drift velocity $U_{d,eff}/(gD)^{1/2}$ is plotted in Fig. 4. The bars cover the range of variation of the results calculated for different flow rates at a given inclination angle β. It can be clearly observed that for the small pipe diameter (Fig. 4(a)) $U_{d,eff}$ are similar to those of single elongated bubbles, while for the larger pipe diameter (Fig. 4(b)) a substantial difference is observed. The calculated effective drift velocities compare quite well to the drift velocities in continuous slug flow obtained by extrapolation (Fig. 9).

The effective translational velocities of elongated bubbles are plotted together with the measured translational velocities in Figs. 6 and 7. It can be seen that the calculated effective translational velocities $U_{tr,eff}$ compare well to the measured ones.

For the smaller pipe diameter in our experiments ($D = 0.024$ m), no significant difference between the translational velocities of single elongated bubble and those in continuous slug flow was observed for all pipe inclinations. The application of the Nicklin correlation (6) for the continuous slug flow is thus justified in this case. This result is supported by the simple model derived here. According to this model, the effect of the dispersed bubbles is negligible if either $\alpha_S \to 0$ or the propagation velocities of elongated and dispersed bubbles are almost the same. Note that for the small pipe diameter $U_d < U_0$ while for $D = 0.054$ m $U_d > U_0$ at all inclinations.

These conditions are not satisfied for the larger diameter pipe ($D = 0.054$ m), see Table 1. Application of the Nicklin correlation (6) in this case is not justified. The suggested model allows calculating the required correction to the translational velocity.

5. Conclusions

The translational velocities of elongated bubbles in continuous inclined slug flow were measured by multiple optical fiber probes and image processing technique in two different pipe diameters. The results were compared to velocities predicted by commonly used empirical correlations. For the smaller pipe diameter, correlation (6) with $C = 1.2$ and U_d according to Eq. (4) predicts quite well the translational velocities of elongated bubbles in continuous slug flow for all pipe inclinations. For the larger pipe diameter, the agreement holds only for a slightly inclined pipe ($\beta < 20°$), while for larger values of β a substantial discrepancy (up to 50%) is observed between the results of Eq. (6) and the measured values. This discrepancy attains a maximum at $\beta \approx 70°$.

It is suggested that the application of the drift velocity of single elongated bubbles to continuous slug flow is inappropriate. This is supposed to be caused by the presence of dispersed bubbles in the liquid slug ahead of the elongated bubble, which may be absorbed by the propagating elongated bubble, yielding an effectively higher translational velocity. A simple model to account for this effect is proposed. The calculated effective translational velocities according to the model are within 15% of the measured translational velocities of elongated bubbles in continuous slug flow.

Acknowledgements

This work was supported by a grant from the Israel Science Foundation. The authors gratefully acknowledge this support.

References

Alves, I.N., Shoham, O., Taitel, Y., 1993. Drift velocity of elongated bubbles in inclined pipes. Chem. Eng. Sci. 48, 3063–3070.

Barnea, D., 1990. Effect of bubble shape on pressure drop calculations in vertical slug flow. Int. J. Multiphase Flow 16, 79–89.

Barnea, D., Brauner, N., 1985. Holdup of the liquid slug in two phase intermittent flow. Int. J. Multiphase Flow 11, 43–49.

Barnea, D., Shemer, L., 1989. Void fraction measurements in vertical slug flow: applications to slug characteristics and transition. Int. J. Multiphase Flow 15, 495–504.

Bendat, J.S., Piersol, A.G., 1968. Measurement and Analysis of Random Data. Wiley, NY.

Bendiksen, K.H., 1984. An experimental investigation of the motion of long bubbles in inclined tubes. Int. J. Multiphase Flow 10, 467–483.

Benjamin, T.B., 1968. Gravity currents and related phenomena. J. Fluid Mech. 31, 209–248.

Bonnecaze, R.H., Eriskine Jr., W., Greskovich, E.J., 1971. Holdup and pressure drop for two-phase slug flow in inclined pipelines. AIChE J. 17, 1109–1113.

Brodkey, R.S., 1967. The Phenomena of Fluid Motions. Addison-Wesley, Reading, MA.

Carew, P.S., Thomas, N.H., Johnson, A.B., 1995. A physically based correlation for the effects of power law rheology and inclination on slug bubble rise velocity. Int. J. Multiphase Flow 21, 1091–1106.

Draper, N.R., Smith, H., 1998. Applied Regression Analysis, third ed. Wiley, NY.

Dumitrescu, D.T., 1943. Strömung an einer Luftblase im senkrechten Rohr. Z. Angew. Math. Mech. 23, 139–149.

Fernandes, R.C., Semiat, R., Dukler, A.E., 1983. Hydrodynamic model for gas–liquid slug flow in vertical tubes. AIChE J. 29, 981–989.

Harmathy, T.Z., 1960. Velocity of large drops and bubbles in media of infinite or restricted extent. AIChE J. 6, 281–288.

Hasan, A.R., Kabir, C.S., 1986. Predicting multiphase flow behavior in a deviated well. 61st Annu. Tech. Conf. New Orleans, La. SPE 15449.

Legius, H.J.W.M., van den Akker, H.E.A., Narumo, T., 1997. Measurements on wave propagation and bubble and slug velocities in cocurrent upward two-phase flow. Exp. Therm. Fluid Sci. 15, 267–278.

Mao, Z.S., Dukler, A.E., 1989. An experimental study of gas–liquid slug flow. Exp. Fluids 8, 169–182.

Nicklin, D.J., Wilkes, J.O., Davidson, J.F., 1962. Two-phase flow in vertical tubes. Trans. Instn. Chem. Engrs. 40, 61–68.

Polonsky, S., Shemer, L., Barnea, D., 1999. The relation between the Taylor bubble motion and the velocity field ahead of it. Int. J. Multiphase Flow 25, 957–975.

Shemer, L., Barnea, D., 1987. Visualization of the instantaneous velocity profiles in gas–liquid slug flow. PhysicoChem. Hydrodyn. 8, 243–253.

Taitel, Y., Barnea, D., 1990. Two-phase slug flow. Adv. Heat Transfer 20, 83–132.

van Hout, R., 2001. Evolution of hydrodynamic and statistical parameters in gas–liquid undeveloped slug flow. Ph.D. thesis, Tel-Aviv University.

van Hout, R., Shemer, L., Barnea, D., 1992. Spatial distribution of void fraction within the liquid slug and some other related slug parameters. Int. J. Multiphase Flow 18, 831–845.

van Hout, R., Barnea, D., Shemer, L., 2001. Evolution of statistical parameters of gas–liquid slug flow along vertical pipes. Int. J. Multiphase Flow 27, 1579–1602.

Wallis, G.B., 1969. One-dimensional Two-phase Flow. McGraw-Hill, New York.

Weber, M.E., Alarie, A., Ryan, M.E., 1986. Velocities of extended bubbles in inclined tubes. Chem. Eng. Sci. 41, 2235–2240.

Zukoski, E.E., 1966. Influence of viscosity, surface tension, and inclination angle on the motion of long bubbles in closed tubes. J. Fluid Mech. 25, 821–837.